

# Comparative Study of Poly(L-Lactic Acid) Scaffolds Coated with Chitosan Nanoparticles Prepared via Ultrasonication and Ionic Gelation Techniques

Majid Salehi<sup>1\*</sup>, Mahdi Naseri-Nosar<sup>1</sup>, Mahmoud Azami<sup>1</sup>, Saeedeh Jafari Nodooshan<sup>2</sup>, Javad Arish<sup>3</sup>

<sup>1</sup>Department of Tissue Engineering and Applied Cell Sciences, School of Advanced Technologies in Medicine, Tehran University of Medical Sciences, Tehran, Iran

<sup>2</sup>Department of Medical Biotechnology, School of Advanced Technologies in Medicine, Tehran University of Medical Sciences, Tehran, Iran

<sup>3</sup>Department of Nanotechnology, School of New Sciences and Technology, Pharmaceutical Sciences Branch of Islamic Azad University, Tehran, Iran

In this study, an attempt was made to develop bi-functional constructs serving both as scaffolds and potential delivery systems for application in neural tissue engineering. The constructs were prepared in two steps. In the first step, the bulks of poly (L-lactic acid) (PLLA) in 1, 4-dioxane/water (87:13) were fabricated using liquid-liquid thermally induced phase separation technique. In the next step, the prepared bulks were coated with chitosan nanoparticles produced by two different techniques of ultrasonication and ionic gelation by grafting-coating technique. In ultrasonication technique, the chitosan solution (2 mg/mL) in acetic acid/sodium acetate buffer (90:10) was irradiated by an ultrasound generator at 20 kHz and power output of 750 W for 100 s. In ionic gelation technique, the tripolyphosphate in water solution (1 mg/mL) was added to the same chitosan solution. The physicochemical properties of the products were characterized by Scanning Electron Microscopy, Attenuated Total Reflection Fourier Transform-Infrared, liquid displacement technique, contact angle measurement, compressive and tensile tests, as well as zeta potential and particle size analysis using dynamic light scattering. Moreover, the cell proliferation and attachment on the scaffolds were evaluated through human glioblastoma cell line (U-87 MG) and human neuroblastoma cell line [BE (2)-C] culture respectively. The results showed that the samples coated with chitosan nanoparticles prepared by ultrasonication possessed enhanced hydrophilicity, biodegradation and cytocompatibility compared with pure PLLA and PLLA coated with chitosan nanoparticles prepared by ionic gelation. This study suggests successful nanoparticles-scaffold systems which can act simultaneously as potential delivery systems and tissue engineering scaffolds. *Tissue Eng Regen Med* 2016;13(5):498-506

**Key Words:** Neural tissue engineering; Poly(L-Lactic acid); Thermally induced phase separation; Chitosan nanoparticles; Ultrasonication; Ionic gelation

## INTRODUCTION

The inability of the adult central nervous system to regenerate itself after a trauma or disease is a challenging issue for neurobiologists and neurologists. Although nerve grafting is the gold standard for neural repair, the challenges in providing autologous donor material or the problems with allograft rejection, caused other alternative methods such as tissue engineering be highly under investigation [1]. Tissue engineering aims to restore the structure and function of defective or damaged tissues mainly via

scaffolds, cells and growth factors [2]. The scaffolds are prepared from natural and/or synthetic materials and act as a temporary environment for cellular attachment, proliferation, migration and differentiation [3]. It is well known that a successful tissue engineering scaffold should be able to carry and release bioactive molecules, such as growth factors, in order to support and improve the attachment, proliferation and differentiation of cells [4]. A number of strategies for controlled biomolecules delivery from scaffolds have been developed for tissue engineering [5]. One common strategy is coating the prefabricated scaffolds with nanoparticles as carriers for delivering therapeutic peptides, proteins, antigens, oligonucleotides and genes. A wide range of materials, such as natural and synthetic polymers, lipids, and surfactants, have been employed to prepare nanoparticles [6,7]. Among them, chitosan due to its outstanding physical and biological properties have received increasing

**Received:** September 18, 2015

**Revised:** December 11, 2015

**Accepted:** December 18, 2015

**\*Corresponding author:** Majid Salehi, Department of Tissue Engineering and Applied Cell Sciences, School of Advanced Technologies in Medicine, Tehran University of Medical Sciences, Tehran 1417755469, Iran.

Tel: 98-9302655158, Fax: 98-2188991117

E-mail: majidsalehi\_ezd@yahoo.com

attention [8]. Chitosan has been widely used in pharmaceutical and medical applications, because of its favorable biological properties such as biodegradability, biocompatibility, low toxicity and good characteristics for attachment, proliferation and viability of cells [9,10]. Besides, cationic nature of chitosan is primarily responsible for electrostatic interactions with negatively charged molecules such as glycosaminoglycans, proteoglycans and growth factors. This property allows chitosan to retain and concentrate the large amount of biomolecules on its structure [11]. It was also shown that chitosan promotes survival and neurite outgrowth of neural cells *in vitro* [12].

Nowadays, the chitosan nanoparticles are prepared by exploiting various techniques such as ultrasonication and ionic gelation [13,14]. Ultrasonication arises from acoustic cavitation phenomenon which causes the formation, growth and collapse of bubbles in a liquid medium. Cavitation can generate very large shear forces through two mechanisms: It generates rapid streaming of solvent molecules around the cavitation bubbles and generates shock waves during bubble collapse [15]. These shear forces in chitosan solution cause the scissions at the 1, 4-glycosidic bond in molecular level and breaking up aggregates and reducing the size of nanoparticles in higher level [13,16].

Ionic gelation is based on the formation of inter- and intramolecular crosslinkage between cationic chitosan molecules and polyanions [17]. Among polyanions, tripolyphosphate (TPP) is widely used in biological applications because of its non-toxic property and quick gelling ability [18]. The chitosan nanoparticles here are made based on interactions between positively-charged chitosan amino groups ( $-\text{NH}_3^+$ ) and negatively-charged TPP ions ( $\text{P}_3\text{O}_{10}^{5-}$ ) at room temperature [19]. Mi et al. [20] proposed that the chitosan-TPP interactions are pH dependent and for ionic gelation to occur, the pH must be below 7. At pH above 7, it may follow another mechanism (coacervation phase-inversion) which is accompanied by light ionic crosslinking.

In the present study, the chitosan nanoparticles as potential delivery systems were prepared by ultrasonication and ionic gelation techniques and coated on Poly(L-lactic acid) (PLLA) bulks produced by liquid-liquid thermally induced phase separation (LL-TIPS) to create bi-functional constructs serving both as scaffolds and delivery systems for exploiting in neural tissue engineering.

## MATERIALS AND METHODS

### Materials

Chitosan ( $M_w=220000$ , 90% deacetylation) was purchased from Eastar holding group (Dongying, China). PLLA with  $M_w=60000$ , acetic acid, tripolyphosphate pentasodium, 1, 4-dioxane, penicillin/streptomycin, gentamicin, phosphate buff-

ered saline (PBS), 3-(4, 5-dimethylthiazol-2-yl)-2, 5-diphenyl-tetrazolium Bromide (MTT) and dimethyl sulfoxide (DMSO) were purchased from Sigma-Aldrich (St. Louis, MO, USA). Sodium acetate buffer was purchased from Merck (Darmstadt, Germany). Aqueous solutions were prepared with de-ionized water. All the chemicals were used as received without further purification.

### Preparation of the bulks

The preparation of PLLA bulks through LL-TIPS method followed the procedure reported by Hua et al. [21]. In brief, PLLA was dissolved in 1, 4-dioxane/water (87:13) on a magnetic stirrer at 60°C for 4 h to prepare 3% (w/v) solutions. The solutions were poured into cylindrical containers and to start liquid-liquid phase separation, they were pre-quenched rapidly from 60°C to 10°C under the expected cloud-point and kept in this temperature for 30 min. Then, the solutions were heated on a magnetic stirrer at 60°C for 30 min and gradually cooled in steps of 1°C to lose their transparent look and become turbid. The cloud-point was determined to be 39°C. The production procedure followed by transferring the scaffolds to a freezer at -40°C for 2 h. The samples then immediately transferred to a freezer dryer at -77°C (Christ, Osterode am Harz, Germany) for 72 h.

### Chitosan nanoparticles preparation

The chitosan nanoparticles were produced using ultrasonication and ionic gelation techniques from 2 mg/mL solution of chitosan in acetic acid/sodium acetate buffer (90:10) at pH=2.4. In ultrasonication technique, the chitosan solution was irradiated by a multiwave ultrasound generator (JY99-IIDN, Scientz, Ningbo, China) at 20 kHz and power output of 750 W for 100 s. In ionic gelation technique, the TPP in water solution (1 mg/mL) at pH=6.95 was added to chitosan solution with the rate of one droplet per min by a syringe pump (SP1000, Fana-varan Nano-Meghyas, Tehran, Iran) under vigorous magnetic stirring at room temperature (the TPP:chitosan weight ratio was 1:3). To coat the bulks with nanoparticles, the PLLA bulks were soaked in acetone/water (70:30) for 1 h, dried at room atmosphere and transferred to each chitosan nanoparticle containing medium for 24 h. The scaffolds then were removed and washed with distilled water for three times.

### Characterization

Particle size and zeta potential of the nanoparticles were determined using Zetasizer (Nano-ZS, Malvern Instruments, Worcestershire, United Kingdom). The analysis was performed for 22 runs at a temperature of 25°C using samples diluted in distilled water with viscosity of 0.8872 cP.

The composition of the scaffolds was evaluated by an Atten-

uated Total Reflection Fourier Transform-Infrared spectroscopy (ATR-FTIR; Nicolet NEXUS 670, Thermo Scientific, Waltham, MA, USA).

The morphology of the scaffolds was observed by a Scanning Electron Microscope (SEM; AIS2100, Seron Technology, Korea) after sputter coating with gold for 180 s using a sputter coater (SC7620, Quorum Technologies, Sussex, United Kingdom) at an accelerating voltage of 20 kV. The liquid displacement method was carried out to determine the porosity of the scaffolds using the following equation [22]. Where  $V_1$  is initial volume of 96% ethanol,  $V_2$  is its volume after scaffold soaking (and ethanol filled the pores) and  $V_3$  is volume of the ethanol after the scaffold removal.

$$\text{Porosity (\%)} = \frac{V_1 - V_3}{V_2 - V_3} \times 100$$

The hydrophilicity of the scaffolds was determined using static contact angle measurements with a sessile drop method by a contact angle measuring system (G10, KRUSS, Hamburg, Germany). Tensile test was performed on dry rectangular samples (30×10 mm) by an Instron 5566 universal testing machine (Instron, Norwood, MA, USA) at a strain rate of 10 mm/min. Compression test was performed on dry cylindrical samples (height and diameter of 25 mm and 20 mm respectively) using a dynamic testing machine (HCT400/25, Zwick/Roell, Ulm, Germany) at a crosshead speed of 0.5 mm/min.

For examining the degradation behavior of the scaffolds, conventional assays follow two methods. One is by measuring the variance in scaffold itself and the other is to measure the degradation products of scaffold. In the present study, monitoring the weight-loss of scaffolds and changes in the pH values of degradation media were employed. The weight-loss of the scaffolds was tested by immersing the samples in 10 mL of three distinct media; distilled water, Dulbecco's modified Eagle's medium (DMEM; Gibco, Grand Island, NY, USA) and DMEM supplemented with 10% (v/v) fetal bovine serum (FBS, Gibco, Grand Island, NY, USA). The initial weights of PLLA bulks were 35 mg and after coating with chitosan nanoparticles their weights elevated to about 40 mg. The weight-loss was calculated using the following equation [23]. Where  $W_1$  is the initial weight of sample and  $W_2$  is the dry weight after removing from the medium.

$$\text{Weight-loss (\%)} = \frac{W_1 - W_2}{W_1} \times 100$$

The changes in the pH values of all samples preserved in normal saline (pH=6.70) at a humidified incubator at 37°C and 5% CO<sub>2</sub>, were measured every week for a total period of 6 weeks by an Inolab pH 720 (WTW, Weilheim, Germany).

### Cell proliferation study

Human glioblastoma cell line (U-87 MG) was purchased from Pasteur Institute National Cell Bank (Tehran, Iran). The cells were cultured in Roswell Park Memorial Institute medium (RPMI; Gibco, Grand Island, NY, USA) supplemented with 10% (v/v) FBS and 1% penicillin/streptomycin in a humidified incubator at 37°C with 5% CO<sub>2</sub>. For scaffold sterilization, 100 µg/mL gentamicin was added to the scaffolds and removed after 20 min. The scaffolds then were washed with PBS once and irradiated by UV light for 20 min. The scaffolds were transferred to 96-well plate and each seeded with 1×10<sup>4</sup> sixth passage cells. Cell proliferation was investigated by MTT assay after 48 h of incubation. The media on cells was removed from each well and 0.01 mL of 5 mg/mL MTT in PBS plus 0.09 mL fresh media was added. The cells then were incubated at 37°C for 4 h. The formed purple formazan crystals were dissolved by adding 0.1 mL DMSO. The absorption was read at 570 nm using a microplate reader (Stat fax-2100, Awareness Technology Inc., Palm City, FL, USA). The U-87 MG cells were treated identically in the rest wells of the plate without scaffolds as negative control. The mean for the triplicate wells for each specimen was reported.

### Cell morphology study

Human neuroblastoma cell line [BE (2)-C] was purchased from Pasteur Institute National Cell Bank. The cells were cultured in RPMI supplemented with 10% (v/v) FBS in a humidified incubator at 37°C with 5% CO<sub>2</sub>. For scaffold sterilization, the samples were immersed in 80% ethanol for 2 h, dried under vacuum for 24 h and irradiated by UV light for 2 h. Then, the scaffolds were transferred to 96-well plate and each seeded with 1×10<sup>4</sup> third passage cells. The media were changed every 24 h. Three days after cell seeding, the cells on the scaffolds were fixed by 2.5% glutaraldehyde for 2 h at room temperature and were dehydrated in a series of increasing concentrations of ethanol in distilled water (30%, 70%, 80%, 90%, and 100%) for 10 min per each concentration. The samples were freeze dried for 24 h and after sputter-coating observed under the SEM.

### Statistical analysis

The results were statistically analyzed by Minitab 17 software using Student's t-test and the data were expressed as mean±SD, n≥3. In all evaluations,  $p < 0.05$  was considered as statistically significant.

## RESULTS

### Particle size analysis and zeta potential of chitosan nanoparticles

The zeta potential values and the mean sizes of chitosan

nanoparticles prepared by ultrasonication (USCN) and ionic gelation (IGCN) are shown in Table 1. Nanoparticles in both techniques were positively charged in accordance to the cationic nature of chitosan. The observed difference between the mean particle sizes of IGCN ( $688.66 \pm 43.55$  nm) and USCN ( $538.33 \pm 176.92$  nm) was attributed to the presence of TPP anions in IGCN. However, the difference was not statistically significant.

## Chemical, physical, and mechanical characterization of the scaffolds

### ATR-FTIR

Soaking the PLLA in water containing media such as this study, causes the hydrolysis to break some of the ester groups on its surface and yields carboxylic acid (-COOH) and hydroxyl (-OH) groups on the PLLA chain termini [24]. The grafting-coating is a process in which the chitosan grafts on the surface of the PLLA by forming amide bonds with these carboxyl groups or by forming hydrogen bonds with PLLA carbonyl groups. Some un-grafted chitosan chains also are entangled and intertwined physically with these grafted chitosan [25-27]. To assess the composition of the coatings, ATR-FTIR analysis was carried out on the samples. From the Figure 1, three distinctive peaks of the PLLA IR spectrum including carbonyl group stretching vibration band at  $1717\text{ cm}^{-1}$  and the ester groups of the backbone at  $1105\text{ cm}^{-1}$  and  $1022\text{ cm}^{-1}$  are visible [28]. Compared with the PLLA, the spectra of PLLA+USCN and PLLA+IGCN presented three characteristic bands of chitosan around  $1540\text{ cm}^{-1}$ ,  $1648\text{ cm}^{-1}$ , and  $901\text{ cm}^{-1}$  assigned to the N-H bending vibration of amide II, the carbonyl stretching of amide I band and the special absorbance peak of  $\beta$ -1,4 glycoside bond in chitosan respectively [29]. However, in the spectrum of PLLA+IGCN, the peak of N-H bending vibration of amide II and the carbonyl stretching of amide I shifted to  $1390\text{ cm}^{-1}$  and  $1412\text{ cm}^{-1}$  respectively as a result of linking between triphosphoric groups of TPP and ammonium groups of chitosan in nanoparticles [30,31]. The N-H bending vibration and the carbonyl stretching bands in the coated samples also can indicate the amide bonds formed between carboxyl groups in hydrolyzed PLLA and chitosan amino groups. The interactions between PLLA and chitosan resulted in the declination of the peak around  $1380\text{ cm}^{-1}$  and the peak between  $2845\text{ cm}^{-1}$  and  $3000\text{ cm}^{-1}$  which are the C-H bending and stretching vibration bands of the alkyl groups respectively. Furthermore, hydrogen bonding between PLLA carbonyls and the chitosan amino groups reduced the intensity of PLLA carbonyl stretching band at  $1730\text{ cm}^{-1}$  [27]. Between the two coated samples, these reductions were more drastic in PLLA+USCN sample which indicates the higher in-

teractions occurred between PLLA and chitosan in this scaffold. Finally, the coatings reduced the crystallization of PLLA bulks. This reduction showed itself by attenuating the crystalline sensitive band of PLLA at  $730\text{ cm}^{-1}$ .

### Morphology of the scaffolds

Figure 2 shows the morphology of all scaffolds. SEM images illustrated that the LL-TIPS method utilized in this study, resulted in the formation of highly porous scaffolds. The pores were interconnected and had almost spherical shapes with the diameters of about  $70\text{ }\mu\text{m}$ . It is possible to distinguish chitosan nanoparticles which heterogeneously aggregated on the constructs and formed a layer of chitosan on the pore walls.

### Porosity measurement

It is generally accepted that the percentage of porosity above 80% is appreciable for the better cell growth [32]. The Porosity of the uncoated PLLA scaffold was calculated about 94%. Soaking the PLLA bulks into chitosan nanoparticle containing media decreased their porosity to 83.50% and 80.20% for PLLA+USCN and PLLA+IGCN samples respectively. We hypothesize

**Table 1.** Mean size and zeta potential values  $\pm$ SD (n=3 in each group) of chitosan nanoparticles prepared by ultrasonication (USCN) and ionic gelation (IGCN) techniques

Method	Mean particle size (nm)	Zeta potential (mV)
USCN	$538.33 \pm 176.92$	$17.80 \pm 2.12$
IGCN	$688.66 \pm 43.55$	$16.54 \pm 0.37$

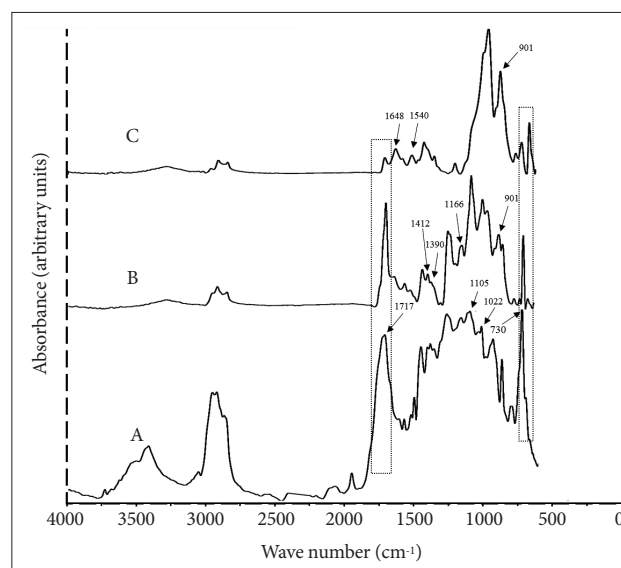


**Figure 1.** ATR-FTIR spectra of (A) PLLA, (B) PLLA+IGCN, and (C) PLLA+USCN. ATR-FTIR: Attenuated Total Reflection Fourier Transform-Infrared, PLLA: poly (L-lactic acid), IGCN: chitosan nanoparticles produced by ionic gelation, USCN: chitosan nanoparticles produced by ultrasonication.

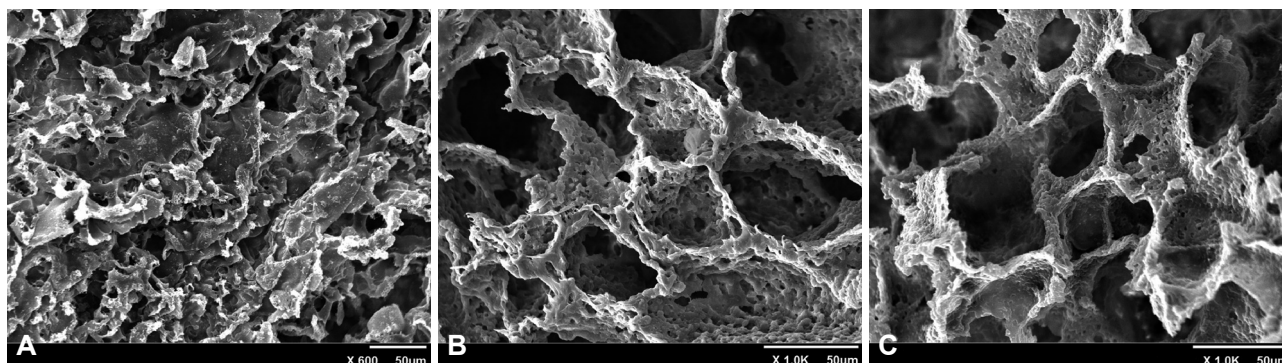


**Figure 2.** SEM images of the scaffolds (A) PLLA, (B) PLLA+USCN, and (C) PLLA+IGCN. SEM: scanning electron microscope, PLLA: poly (L-lactic acid), USCN: chitosan nanoparticles produced by ultrasonication, IGCN: chitosan nanoparticles produced by ionic gelation.

that this reduction can be attributed to the microstructural deformation occurred by soaking the PLLA bulks into the media and nanoparticles tendency to aggregate and form larger clusters and filling the small pores. In PLLA+IGCN scaffold, this aggregation led to further decrease in porosity compared with PLLA+USCN because of the larger particles of IGCN. Nevertheless, all the scaffolds met the demands of porosity for desired scaffolds and hence it is expected that they would act as an ideal place for cell growth.

**Contact angle measurement**

The contact angles of all samples were assessed by Zisman method (Table 2). PLLA has been widely used in tissue engineering due to its excellent biodegradability and nontoxicity of the degradation products. However, methyl groups (CH<sub>3</sub>) in this polymer by having lower binding energy make it highly hydrophobe and limit its utility [33]. Chitosan grafting is a common way to enhance hydrophilicity [34]. Coating the PLLA with chitosan nanoparticles, decreases its hydrophobicity by the means of amino and hydroxyl groups on chitosan chains. In our work, presence of nanoparticles evidently decreased the contact angle from 99° in uncoated PLLA scaffold to about 62° in coated samples. Between PLLA+USCN and PLLA+IGCN scaffolds, no significant difference was observed.

**Mechanical properties**

Tensile strength and compressive modulus of all samples are shown in Table 3. Reduction in the tensile strength of coated scaffolds compared with uncoated PLLA scaffold is due to the thermodynamic immiscibility and inherent incompatibility between chitosan and PLLA [35]. Very low interfacial adhesion between the chitosan and PLLA, caused at the lower stress the debonding occurred when the load was applied to the coated scaffolds [36]. The higher interactions between PLLA and chitosan in PLLA+USCN compared with PLLA+IGCN observed earlier in ATR-FTIR test, made the tensile strength

**Table 2.** The contact angle measurement of all scaffolds

Sample	Contact angle (°)
PLLA 3% (w/v)	98.80±0.52
PLLA 3% (w/v)+USCN	61.90±0.14*
PLLA 3% (w/v)+IGCN	62.15±0.12***

Mean contact angle values±SD (n=3 in each group) are significantly different. \**p*<0.05, \*\*\**p*<0.005 compared with PLLA 3% (w/v). PLLA: poly (L-lactic acid), USCN: chitosan nanoparticles produced by ultrasonication, IGCN: chitosan nanoparticles produced by ionic gelation

**Table 3.** The compressive and tensile properties of all scaffolds

Sample	Compressive modulus (MPa)	Tensile strength (MPa)
PLLA 3% (w/v)	1.60±0.11	3.10±0.22
PLLA 3% (w/v)+USCN	2.60±0.26	2.92±0.12
PLLA 3% (w/v)+IGCN	2.80±0.17	2.89±0.12

Mean compressive modulus and tensile strength values±SD (n=3 in each group). There is no statistically significant difference in compressive modulus and tensile strength of scaffolds. PLLA: poly (L-lactic acid), USCN: chitosan nanoparticles produced by ultrasonication, IGCN: chitosan nanoparticles produced by ionic gelation

of PLLA+USCN scaffold higher than PLLA+IGCN. However, the difference in their tensile strength was not significant.

Compression test is widely accepted to evaluate the mechanical strength of tissue engineering scaffolds [37-39]. It can be seen that the compressive modulus of coated scaffolds were higher than that of pure PLLA, which means the chitosan reinforced the PLLA bulks to some extent. However, there was no statistically significant difference in the compressive modulus of PLLA+USCN and PLLA+IGCN scaffolds. The reinforcement role of chitosan in the coated scaffolds here can be attributed to its role in decreasing the porosity. It is well accepted that the compressive modulus of the scaffold increases with decreasing the porosity [40].

**Table 4.** Weight-loss measurement of all scaffolds in distilled water, DMEM and 90% DMEM/10% FBS for 60 days

Sample	Media	Weight-loss after 30 days (%)	Weight-loss after 60 days (%)
PLLA 3% (w/v)	Distilled water	0	0
	DMEM	1.70	2.30
	90% DMEM/10% FBS	24.40	28.20
PLLA 3% (w/v)+USCN	Distilled water	9.80	25
	DMEM	15.70	27
	90% DMEM/10% FBS	38	64
PLLA 3% (w/v)+IGCN	Distilled water	9.57	20
	DMEM	16.20	29
	90% DMEM/10% FBS	40	64.60

PLLA: poly (L-lactic acid), USCN: chitosan nanoparticles produced by ultrasonication, IGCN: chitosan nanoparticles produced by ionic gelation, DMEM: Dulbecco's modified Eagle's medium, FBS: fetal bovine serum

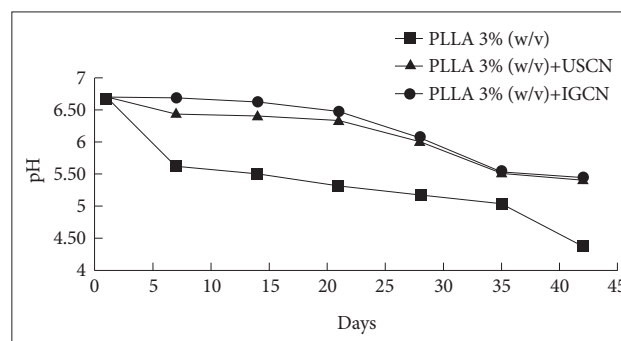
### In vitro degradation of scaffolds

Table 4 provides the results of weight-loss measurement. The measurement was carried out for 60 days in three media (distilled water, DMEM and 90% DMEM/10% FBS). During this time, the media were exchanged with fresh ones every week. In each interval (every 30 days), the samples were removed from the media, rinsed with distilled water, dried under vacuum and their weights were measured. No significant difference was observed in the weight-loss between PLLA+USCN and PLLA+IGCN scaffolds. The results also showed that the weight-loss of all scaffolds after 30 and 60 days in the second (DMEM) and third medium (90% DMEM/ 10% FBS) were higher than distilled water. The higher degradation in DMEM medium can be justified by considering the complexity of its composition: inorganic salts, amino acids, vitamins and others [41] and presence of enzymes in FBS caused the scaffolds in the third medium to experience the highest weight-loss.

The pH changes were monitored every seven days for six weeks (Fig. 3). Hydrolytic degradation of steric bonds in PLLA resulted in non-toxic byproducts of mainly lactic acid which decreased the pH value drastically from 6.7 to 5.5 after two weeks. The pH value of the PLLA+USCN and PLLA+IGCN decreased slowly from 6.7 to 6.44 and 6.68 respectively in the same time period.

### Cell proliferation and attachment study

MTT assay was carried out to evaluate the proliferation of U-87 MG cells on the scaffolds and the results were shown in Figure 4. After two days of incubation, it can be seen that the chitosan containing scaffolds, because of their higher hydrophilicity, showed higher cell proliferation compared with the pure PLLA scaffold. Besides, the cationic nature of chitosan encouraged the cell attachment and proliferation due to the negative charge of the cell surface [23]. Comparing two chitosan con-



**Figure 3.** pH values of all scaffolds in the normal saline as a function of the degradation time. PLLA: poly (L-lactic acid), IGCN: chitosan nanoparticles produced by ionic gelation, USCN: chitosan nanoparticles produced by ultrasonication.

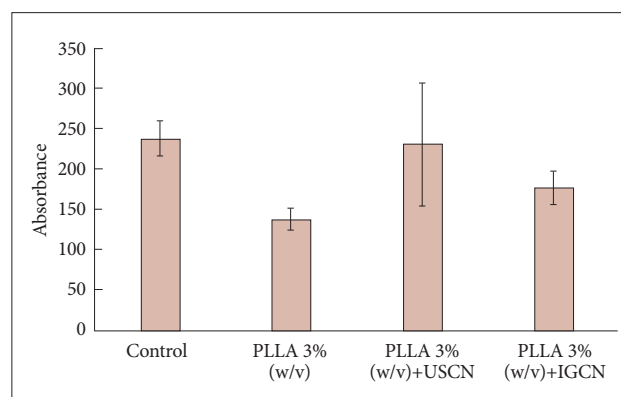


**Figure 4.** MTT assay for the U-87 MG cells seeded onto control, PLLA, PLLA+USCN, and PLLA+IGCN. The data are expressed as mean±SD, n=3. There is no statistically significant difference between each scaffold and control. MTT: (3-(4, 5-dimethylthiazol-2-yl)-2,5-diphenyltetrazolium bromide), PLLA: poly (L-lactic acid), IGCN: chitosan nanoparticles produced by ionic gelation, USCN: chitosan nanoparticles produced by ultrasonication.

taining scaffolds, the PLLA+USCN showed higher cell proliferation which can be linked to the higher hydrophilicity of this scaffold compared with PLLA+IGCN.

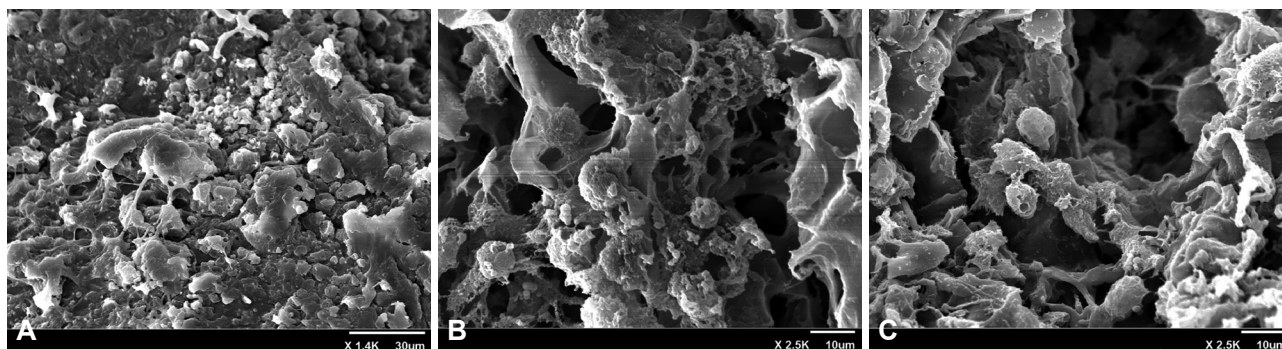


**Figure 5.** SEM images of the BE (2)-C cells attached on the scaffolds (A) PLLA, (B) PLLA+USCN, and (C) PLLA+IGCN. SEM: scanning electron microscope, PLLA: poly (L-lactic acid), USCN: chitosan nanoparticles produced by ultrasonication, IGCN: chitosan nanoparticles produced by ionic gelation.

After 3 days, the BE (2)-C cells morphology on the scaffolds was observed by SEM (Fig. 5). The cells on all three scaffolds showed almost the same morphology. The cells were primarily present in the superficial area of the scaffolds and showed poor spreading tendency and maintained their spherical morphology with some short processes and lamellipodia. We hypothesize that this low tendency in coated samples originated from the dissolution of chitosan nanoparticle layer in cell culture medium. High cellular proliferation of BE (2)-C cells and changing the culture media every 24 h caused the media to become acidic before changing with fresh one. This acidic condition dissolved parts of surface chitosan layer and exposed PLLA bulk to cells and made the interactions of cells with the coated surfaces almost similar to uncoated PLLA scaffold.

## DISCUSSION

The observed difference between the mean particle sizes of IGCN and USCN can be attributed to the presence of TPP anions in the IGCN structure. Unlike the USCN preparation, which the ultrasonication breaks the 1, 4-glycosidic bonds and dissociate chitosan aggregates (which were formed due to the Brownian motion of the particles and attached because of adhesive nature of chitosan [42]), the TPP acts as a curing agent and crosslinks chitosan chains together and subsequently made larger particles [43,44]. The smaller positive zeta potential of IGCN compared with USCN was related to the TPP anions in their structure. However, the presence of TPP mainly in the bulk of the chitosan nanoparticles, caused the IGCN did not experience a drastic decrease in their zeta potential value [43].

It was expected that the smaller mean particle size and higher zeta potential of USCN make the contact angle of PLLA+USCN sample significantly smaller than PLLA+IGCN. However, the ladder-like conformation of chitosan chains in chitosan+TPP complex prepared in acidic media (Fig. 6), caused the intermolecular hydrogen bonding of ammoniums to restrain and be-

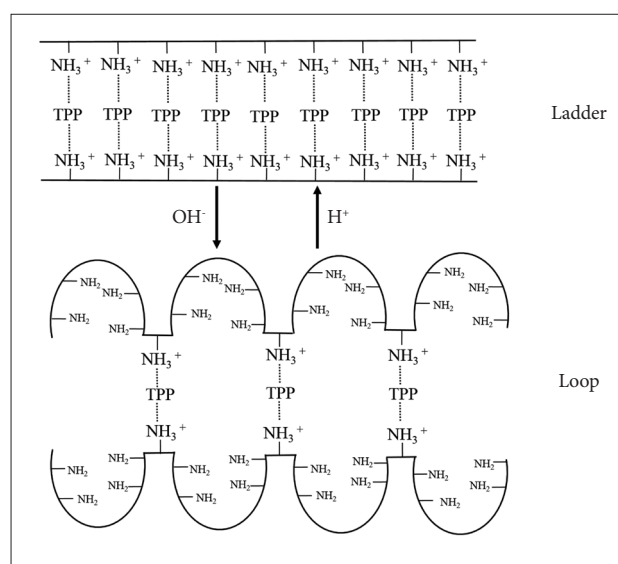


**Figure 6.** Ladder-loop transition of chitosan-TPP complex structures. TPP: triphosphosphate.

come exposed more to water molecules and increase the hydrophilicity of PLLA+IGCN scaffold [43,44].

PLLA is an aliphatic polyester, which degrades mainly through hydrolysis of the hydrolytically sensitive ester linkage in the polymer's backbone into lactic acid [45,46]. Chitosan is generally degrades through lysozyme-mediated system by randomly cleaving glucosamine and N-acetyl glucosamine oligomers [37]. Lysozyme mediated degradation of chitosan can be beneficial in neural tissue engineering applications. Lysozyme was reported to be synthesized during active phagocytosis after nerve injury. Thus, it will be available for the degradation of chitosan contained scaffolds [12]. In the lysozyme free systems such as this study, chitosan degradation hardly occurs alone and the observed weight-loss was related to chitosan dissolution in water (our chitosan was partially water soluble). Although, López-León et al. [47] reported that chitosan nanoparticles prepared by ionic gelation technique with TPP, lose their integrity in aque-

ous media even in the absence of enzymes, the biodegradation here should be mainly ascribed to the degradation of PLLA. Chen et al. [48] reported that the PLLA scaffolds degradation rate significantly enhanced after chitosan grafting. Consistently, we observed the weight-loss of PLLA bulks increased significantly after coating with chitosan nanoparticles. This may be due to the following reasons. First, while the PLLA degradation is mainly by the hydrolysis of ester groups, coating with chitosan nanoparticles increased its hydrophilicity and consequently further interaction with water. Second, incorporation of chitosan nanoparticles can increase the number of small crystallites and then lower the overall crystallinity of PLLA which was observed earlier in ATR-FTIR test. Since the biodegradation takes place first in the amorphous regions and then, the reaction zone moves to crystalline regions in most semi-crystalline biodegradable polymers, reduction in the overall crystallinity of PLLA led to increase in biodegradation of coated scaffolds [49].

The pH value of the PLLA+IGCN during degradation decreased more slowly compared with PLLA+USCN. It was expected because the chitosan is a weakly basic polymer and the fragments and oligomers released from the chitosan chains during the dissolution and degradation would increase pH of the media [50]. In fact, the alkaline groups in chitosan (i.e., amino groups) can neutralize the acidic degradation products of PLLA. Therefore, the pH reduction curve of the coated scaffolds declined more slowly than that of the uncoated one. This improved lower acidity atmosphere is favorable for reducing the inflammatory reactions during the application of the scaffolds [51]. In PLLA+IGCN scaffold, the buffer ability of TPP ions in weak acids resulted in a moderate decrease of pH values for the first three weeks. After this period, the pH decreased similar to PLLA+USCN scaffold. It was suggested that the TPP ions lose their buffer ability due to binding to the protonated chitosan [44]. However, the dominant content of PLLA in both coated scaffolds, made their total pH reduction trends similar to each other.

### Acknowledgements

This research was supported by Tehran University of Medical Sciences (grant number: 93-01-87-25315).

### Conflicts of Interest

The authors have no financial conflicts of interest.

### Ethical Statement

There are no animal experiments carried out for this article.

### REFERENCES

- Schmidt CE, Leach JB. Neural tissue engineering: strategies for repair and regeneration. *Annu Rev Biomed Eng* 2003;5:293-347.
- Kessler MW, Grande DA. Tissue engineering and cartilage. *Organogenesis* 2008;4:28-32.
- Duarte ARC, Mano JF, Reis RL. Preparation of starch-based scaffolds for tissue engineering by supercritical immersion precipitation. *J Supercrit Fluids* 2009;49:279-285.
- Zhu N, Li MG, Cooper D, Chen XB. Development of novel hybrid poly(L-lactide)/chitosan scaffolds using the rapid freeze prototyping technique. *Biofabrication* 2011;3:034105.
- Tessmar JK, Göpferich AM. Matrices and scaffolds for protein delivery in tissue engineering. *Adv Drug Deliv Rev* 2007;59:274-291.
- Blasi P, Giovagnoli S, Schoubben A, Ricci M, Rossi C. Solid lipid nanoparticles for targeted brain drug delivery. *Adv Drug Deliv Rev* 2007;59:454-477.
- Kumari A, Yadav SK, Yadav SC. Biodegradable polymeric nanoparticles based drug delivery systems. *Colloids Surf B Biointerfaces* 2010;75:1-18.
- Liu Z, Jiao Y, Wang Y, Zhou C, Zhang Z. Polysaccharides-based nanoparticles as drug delivery systems. *Adv Drug Deliv Rev* 2008;60:1650-1662.
- Hejazi R, Amiji M. Chitosan-based gastrointestinal delivery systems. *J Control Release* 2003;89:151-165.
- Muzzarelli RAA. Chitins and chitosans for the repair of wounded skin, nerve, cartilage and bone. *Carbohydrate Polym* 2009;76:167-182.
- Shi C, Zhu Y, Ran X, Wang M, Su Y, Cheng T. Therapeutic potential of chitosan and its derivatives in regenerative medicine. *J Surg Res* 2006;133:185-192.
- Freier T, Koh HS, Kazazian K, Shoichet MS. Controlling cell adhesion and degradation of chitosan films by N-acetylation. *Biomaterials* 2005;26:5872-5878.
- Tang ES, Huang M, Lim LY. Ultrasonication of chitosan and chitosan nanoparticles. *Int J Pharm* 2003;265:103-114.
- Patel JK, Jivani NP. Chitosan based nanoparticles in drug delivery. *Int J Pharm Sci Nanotechnol* 2009;2:517-522.
- Suslick KS, Price GJ. Applications of ultrasound to materials chemistry. *Annu Rev Mater Sci* 1999;29:295-326.
- Chen RH, Chang JR, Shyur JS. Effects of ultrasonic conditions and storage in acidic solutions on changes in molecular weight and polydispersity of treated chitosan. *Carbohydrate Res* 1997;299:287-294.
- Gan Q, Wang T. Chitosan nanoparticle as protein delivery carrier--systematic examination of fabrication conditions for efficient loading and release. *Colloids Surf B Biointerfaces* 2007;59:24-34.
- Gan Q, Wang T, Cochrane C, McCarron P. Modulation of surface charge, particle size and morphological properties of chitosan-TPP nanoparticles intended for gene delivery. *Colloids Surf B Biointerfaces* 2005;44:65-73.
- Ko JA, Park HJ, Hwang SJ, Park JB, Lee JS. Preparation and characterization of chitosan microparticles intended for controlled drug delivery. *Int J Pharm* 2002;249:165-174.
- Mi FL, Shyu SS, Chen CT, Lai JY. Adsorption of indomethacin onto chemically modified chitosan beads. *Polymer* 2002;43:757-765.
- Hua FJ, Kim GE, Lee JD, Son YK, Lee DS. Macroporous poly(L-lactide) scaffold 1. Preparation of a macroporous scaffold by liquid-liquid phase separation of a PLLA-dioxane-water system. *J Biomed Mater Res* 2002;63:161-167.
- Ho ST, Huttmacher DW. A comparison of micro CT with other techniques used in the characterization of scaffolds. *Biomaterials* 2006;27:1362-1376.
- Salehi M, Nosar MN, Amani A, Azami M, Tavakol S, Ghanbari H. Preparation of pure PLLA, pure chitosan, and PLLA/chitosan blend porous tissue engineering scaffolds by thermally induced phase separation method and evaluation of the corresponding mechanical and biological properties. *Int J Polym Mater Polym Biomater* 2015;64:675-682.
- Lao L, Tan H, Wang Y, Gao C. Chitosan modified poly(L-lactide) microspheres as cell microcarriers for cartilage tissue engineering. *Colloids*



- Surf B Biointerfaces 2008;66:218-225.
25. Hong Y, Gao C, Xie Y, Gong Y, Shen J. Collagen-coated polylactide microspheres as chondrocyte microcarriers. *Biomaterials* 2005;26:6305-6313.
  26. Liao YZ, Xin MH, Li MC, Su S. Preparation and characterization O-lauroyl chitosan/poly(l-lactic acid) blend membranes by solution-casting approach. *Chin Chem Lett* 2007;18:213-216.
  27. Chen C, Dong L, Cheung MK. Preparation and characterization of biodegradable poly(l-lactide)/chitosan blends. *Eur Polym J* 2005;41:958-966.
  28. Moffa M, Polini A, Sciancalepore AG, Persano L, Mele E, Passione LG, et al. Microvascular endothelial cell spreading and proliferation on nanofibrous scaffolds by polymer blends with enhanced wettability. *Soft Matter* 2013;9:5529-5539.
  29. Peniche C, Argüelles-Monal W, Davidenko N, Sastre R, Gallardo A, San Román J. Self-curing membranes of chitosan/PAA IPNs obtained by radical polymerization: preparation, characterization and interpolymer complexation. *Biomaterials* 1999;20:1869-1878.
  30. Xu Y, Du Y. Effect of molecular structure of chitosan on protein delivery properties of chitosan nanoparticles. *Int J Pharm* 2003;250:215-226.
  31. Wu Y, Yang W, Wang C, Hu J, Fu S. Chitosan nanoparticles as a novel delivery system for ammonium glycyrrhizinate. *Int J Pharm* 2005;295:235-245.
  32. Yang F, Murugan R, Ramakrishna S, Wang X, Ma YX, Wang S. Fabrication of nano-structured porous PLLA scaffold intended for nerve tissue engineering. *Biomaterials* 2004;25:1891-1900.
  33. Zhu X, Cui W, Li X, Jin Y. Electrospun fibrous mats with high porosity as potential scaffolds for skin tissue engineering. *Biomacromolecules* 2008;9:1795-1801.
  34. Thanou M, Verhoef JC, Junginger HE. Oral drug absorption enhancement by chitosan and its derivatives. *Adv Drug Deliv Rev* 2001;52:117-126.
  35. Pukanszk B, Maurer FHJ, Boode JW. Impact testing of polypropylene blends and composites. *Polym Eng Sci* 1995;35:1962-1971.
  36. Correlo VM, Boesel LF, Bhattacharya M, Mano JF, Neves NM, Reis RL. Properties of melt processed chitosan and aliphatic polyester blends. *Mater Sci Eng A* 2005;403:57-68.
  37. Jiao Y, Liu Z, Zhou C. Fabrication and characterization of PLLA-chitosan hybrid scaffolds with improved cell compatibility. *J Biomed Mater Res A* 2007;80:820-825.
  38. Li Z, Ramay HR, Hauch KD, Xiao D, Zhang M. Chitosan-alginate hybrid scaffolds for bone tissue engineering. *Biomaterials* 2005;26:3919-3928.
  39. Zhang Y, Zhang M. Synthesis and characterization of macroporous chitosan/calcium phosphate composite scaffolds for tissue engineering. *J Biomed Mater Res* 2001;55:304-312.
  40. Ma PX, Choi JW. Biodegradable polymer scaffolds with well-defined interconnected spherical pore network. *Tissue Eng* 2001;7:23-33.
  41. Peña J, Corrales T, Izquierdo-Barba I, Doadrio AL, Vallet-Regí M. Long term degradation of poly( $\epsilon$ -caprolactone) films in biologically related fluids. *Polym Degrad Stab* 2006;91:1424-1432.
  42. Li RK, Weisel RD. *Cardiac regeneration and repair*. 1st ed. Cambridge, UK: Woodhead Publishing; 2014.
  43. Nasti A, Zaki NM, de Leonardi P, Ungphaiboon S, Sansongsak P, Rimoli MG, et al. Chitosan/TPP and chitosan/TPP-hyaluronic acid nanoparticles: systematic optimisation of the preparative process and preliminary biological evaluation. *Pharm Res* 2009;26:1918-1930.
  44. Mi FL, Shyu SS, Lee ST, Wong TB. Kinetic study of chitosan-tripolyphosphate complex reaction and acid-resistive properties of the chitosan-tripolyphosphate gel beads prepared by in-liquid curing method. *J Polym Sci B Polym Phys* 1999;37:1551-1564.
  45. Middleton JC, Tipton AJ. Synthetic biodegradable polymers as orthopedic devices. *Biomaterials* 2000;21:2335-2346.
  46. Lu L, Peter SJ, Lyman MD, Lai HL, Leite SM, Tamada JA, et al. In vitro degradation of porous poly(L-lactic acid) foams. *Biomaterials* 2000;21:1595-1605.
  47. López-León T, Carvalho EL, Seijo B, Ortega-Vinuesa JL, Bastos-González D. Physicochemical characterization of chitosan nanoparticles: electrokinetic and stability behavior. *J Colloid Interface Sci* 2005;283:344-351.
  48. Chen S, Hao Y, Cui W. Biodegradable electrospun PLLA/chitosan membrane as guided tissue regeneration membrane for treating periodontitis. *J Mater Sci* 2013;48:6567-6577.
  49. Lee JH, Park TG, Park HS, Lee DS, Lee YK, Yoon SC, et al. Thermal and mechanical characteristics of poly(l-lactic acid) nanocomposite scaffold. *Biomaterials* 2003;24:2773-2778.
  50. Wan Y, Wu H, Cao X, Dalai S. Compressive mechanical properties and biodegradability of porous poly(caprolactone)/chitosan scaffolds. *Polym Degrad Stab* 2008;93:1736-1741.
  51. Wang X, Song G, Lou T, Peng W. Fabrication of nano-fibrous PLLA scaffold reinforced with chitosan fibers. *J Biomater Sci Polym Ed* 2009;20:1995-2002.